

## ***s*-wave photodetachment in a static electric field**

N. D. Gibson, B. J. Davies, and D. J. Larson

*Department of Physics, University of Virginia, Charlottesville, Virginia 22901*

(Received 20 August 1992)

Photodetachment from negative ions in a static electric field has been studied using  $\text{Cl}^-$  and  $\text{S}^-$ . These experiments were done with greater precision than previous studies and allow a quantitative comparison of data with theory. A 10-keV ion beam was sent through a region with fields of up to 1.5 kV/cm applied parallel to the beam velocity. A pulsed dye-laser beam, perpendicular to the ion beam, photoneutralized the ions. The relative cross sections were measured by detecting the resulting fast neutral atoms. Detachment below threshold and oscillations on the cross section above threshold were observed near the  $\text{S}^-$  threshold at  $16\,269.5\text{ cm}^{-1}$  and near the  $\text{Cl}^-$  threshold at  $29\,138.3\text{ cm}^{-1}$ . The phase of the oscillations in the data is in good agreement with predictions for *s*-wave photodetachment in a static electric field, but the amplitude of the oscillations is found to be slightly reduced.

PACS number(s): 32.80.Fb, 32.60.+i

### **I. INTRODUCTION**

The behavior near threshold of cross sections for photodetachment from negative ions has been thoroughly investigated and appears to be well understood. Near threshold, this behavior is described by the Wigner law [1,2]. However, an electric field modifies the zero-field cross section. A constant electric field gives rise to below-threshold detachment as well as oscillations on the cross section above threshold and a nonzero cross section at threshold. These effects can be explained by the use of a model which treats the negative ion as an electron bound in a short-range potential and the detached electron as a free electron in a static field. Below the zero-field threshold, the now finite-width potential barrier on one side of the atom allows the bound electron to tunnel out. Above threshold, part of the wave function of the emerging electron is reflected from the potential slope of the electric field. If the reflection takes less time than the coherence time of the detachment (the time between phase changes in the optical field, collisions, etc.) the reflected part of the wave function will interfere with the part originally propagating down the potential hill, giving rise to oscillations on the cross section.

During the past 12 years, a number of calculations [3–12] have been carried out on the way an electric field modifies photodetachment cross sections. Three experiments have observed such effects. Only one of these experiments was designed to investigate static-electric-field effects. In 1987, Bryant *et al.* reported an observation of the effects of an electric field on a photodetachment cross section [13]. They observed the effect of a motional electric field on the photodetachment cross section of  $\text{H}^-$ . Further work with  $\text{H}^-$  was reported subsequently by the same group (Stewart *et al.* [14] and Harris *et al.* [15]). The data appeared to be in reasonably good agreement with theory, but a careful quantitative comparison of the oscillation amplitudes was not made. Oscillations on the  $\text{Rb}^-$  photodetachment cross section near the  $5p_{1/2}$  threshold were recorded by Frey *et al.* [16,17] in 1978,

but were not understood to be due to an electric field until modeled by Greene and Rouze in 1988 [18]. Green and Rouze point out that the periodicity of the oscillations seems to be in agreement with the model, but that the amplitude of the oscillations is not quantitatively correct. This lack of agreement may be due to the complication of having more than one available detachment channel. More recently, Baruch *et al.* carried out photodetachment experiments in a microwave field [19,20]. The detachment time was short compared to the period of the microwave field, and the results were largely consistent with models for photodetachment in a static electric field modified to account for time averaging of the field amplitude. The averaging reduces the expected oscillations by about a factor of 2, and the quality of the data did not permit precise comparison with theory. So, until now, a careful quantitative comparison of data with theory for *s*-wave photodetachment in a static electric field had not been made.

The purpose of the experiment described in this paper is to acquire better quality data in a truly static field and to resolve questions about possible effects near threshold suggested by the microwave data [20]. As in the experiment with microwave fields, the ratio of the cross section with the electric field on to that with the field off was measured. Measuring this ratio removes normalization errors between the field-on and field-off detachments and largely eliminates effects of the overall shape of the cross section. Thus measuring the ratio provides a very direct test of electric-field effects. The apparatus was designed to have a precise, repeatable static electric field, and single-channel *s*-wave detachment from well-understood negative ions,  $\text{Cl}^-$  and  $\text{S}^-$ , was chosen to keep the experiment simple.

### **II. MODEL**

The model briefly described here is presented in more detail in Baruch *et al.* [20]. Above threshold, the photodetachment cross section in a static electric field can be

expressed in terms of the cross section without the field and an oscillating function  $H(E, F)$  which incorporates the effect of the field,  $F$  [18],

$$\sigma_F = H(E, F)\sigma_{F=0}. \quad (1)$$

Here  $E = E_p - E_a$  is the difference between the photon energy and the electron affinity. When the detaching field is relatively weak,  $H(E, F)$  can be found by using Fermi's "golden rule" to evaluate the cross sections with and without the field. Near threshold, simplifying assumptions can be used to evaluate the matrix elements. For  $s$ -wave detachment, the necessary dipole matrix elements can be calculated using the  $\delta$  function to represent the photon acting on the short-range initial bound state. In the field free case, the final state can be represented by a free-electron wave function. The cross section above threshold is then found to be

$$\sigma_{F=0} = \frac{\sqrt{2}\alpha}{\pi} D E_p E^{1/2}, \quad (2)$$

where  $D$  is a normalization constant,  $\alpha$  is the fine-structure constant, and all values are in atomic units. This is just the  $s$ -wave ( $l=0$ ) case of the more general Wigner law [1],

$$\sigma \propto E^{l+1/2}, \quad (3)$$

which can be obtained from similar arguments.

In the presence of the field, the final state can be represented by that of a free electron in the field. The resulting cross section is

$$\sigma_F = \frac{2^{2/3}\alpha D E_p}{F^{1/3}} \int_{-\infty}^E \left[ \text{Ai} \left( -2^{1/3} \frac{E}{F^{2/3}} \right) \right]^2 dE. \quad (4)$$

$H(E, F)$  is then found by dividing  $\sigma_F$  by  $\sigma_{F=0}$ ,

$$H(E, F) \equiv \frac{\sigma_F}{\sigma_{F=0}} = \pi \frac{F^{1/3}}{2^{1/6} E^{1/2}} \int_{-\infty}^{\gamma_{\max}} \text{Ai}^2(-\gamma') d\gamma', \quad (5)$$

where  $\gamma_{\max} \equiv (2/F^2)^{1/3}(E_p - E_a)$ . For single-channel  $s$ -wave detachment, this model produces the same result as the zero phase-shift limit of the frame transformation theory presented by Wong, Rau, and Greene [11]. Since the data were collected in a manner which records the ratios of the cross section with the field on to the cross section with the field off, direct comparison of the data with  $H(E, F)$  can be made.

### III. EXPERIMENTAL APPARATUS

The experiment was performed using a high-vacuum ion-beam apparatus with a negative-ion sputter source. A pulsed dye-laser beam was overlapped with the ion beam between a set of parallel plates. The amount of detachment was measured using time-resolved counting of the resulting neutral atoms. The remaining ions were electrostatically deflected out of the beam and the neutral atoms were counted using a channeltron detector. The neutral counts were collected in  $1\text{-}\mu\text{s}$ -wide bins using a computer-assisted measurement-and-control (CAMAC)

based data-collection system. Figure 1 illustrates the experimental apparatus.

A SNICS II (source of negative ions by cesium sputtering) was used to produce the ions. The source was manufactured by National Electrostatics Corporation and is usually used to produce 80-keV beams in the 10–100- $\mu\text{A}$  range. This type of source is capable of producing a wide range of different negative ions [21]. The source consists of a spherical tantalum ionizer, which is surrounded by a Cs vapor, and a cathode of the desired ion material. An oven supplies the cesium vapor, a 15–25-A current heats the ionizer in the vacuum, and the atoms are ionized to produce  $\text{Cs}^+$ . The  $\text{Cs}^+$  is then accelerated through a 5-kV potential towards the negatively biased cathode. Upon impact, the cesium sputters atoms off the cathode; those that form negative ions are accelerated away from the cathode and focused into a beam. It is believed that a thin layer of Cs builds up on the cathode surface and enhances the production of negative ions. By floating the ionizer at  $-5$  kV and biasing the cathode 5 kV lower, a 10-keV ion beam is formed.

Since the source produces ions of nearly all species present in the cathode, including impurities such as hydrogen and oxygen, some form of mass analysis is required. Fortunately, the ions are formed on a surface of constant potential and this produces a nearly monoenergetic beam so the velocities of the different ions are inversely proportional to the square roots of their masses. A 10.0-keV beam energy gives  $\text{S}^-$  a velocity of  $2.46 \times 10^7$  cm/s and  $^{35}\text{Cl}^-$  and  $^{37}\text{Cl}^-$  velocities of  $2.35 \times 10^7$  and  $2.28 \times 10^7$  cm/s. This allows the use of a velocity filter to perform mass selection. A Colutron model 300  $\mathbf{E} \times \mathbf{B}$  velocity filter with a 3-in. electromagnet was used with a current of 3.0 A to produce a magnetic field of 570 G.

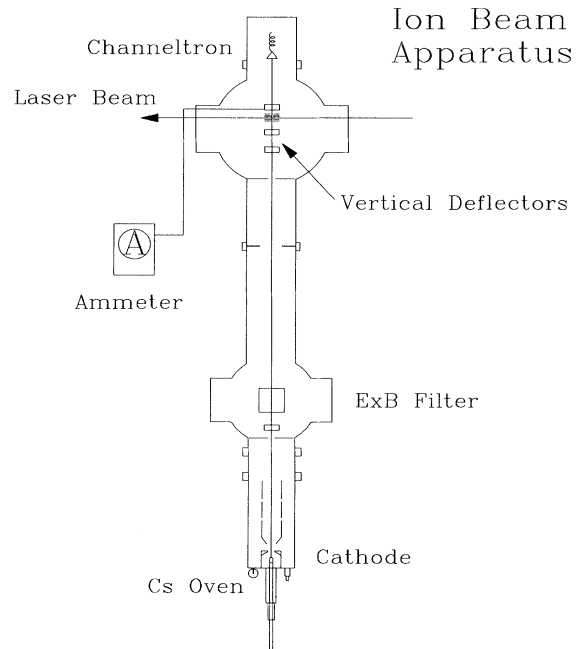


FIG. 1. Experimental apparatus.

Using a drift region of about one meter, this filter provided adequate mass resolution for these experiments.

The laser and ion interaction chamber contains a vertical deflection region and the static-field region. Using a set of charged horizontal plates, the beam is sharply angled upwards immediately before the static-field region in order to separate the ions from the neutrals produced by collisional stripping. A second set of horizontal plates levels the beam and directs the ions through the aperture in the first plate in the static-field region. The background neutrals must be removed from the ion-beam path as close to the photodetachment area as possible since the neutral background detected is proportional to the ion path length through the background gas. At 1 nA and  $2 \times 10^{-7}$  Torr, this configuration produced about  $\frac{1}{2}$  background count per microsecond as compared to photodetachment signals of up to 2 counts per microsecond.

The static-field region consists of a shield plate, two static-field plates, and two more shield plates. The first, fourth, and fifth vertical plates are grounded in order to shield the photodetachment region from stray fields and to reduce the field's effect on the ion beam. The shield plates and field plates are normal to the beam and produce an electric field parallel to the beam. The field plates are 5.08 cm square and each has a 3-mm hole in the center. The second plate is positively charged and the third plate, 1.016 cm away, has a negative charge of equal magnitude. Compared to charging only one plate, this configuration creates a more uniform electric field, produces minimal focusing and deflection of the ion beam, and allows photodetachment in a region of near zero potential relative to the system ground. The maximum electric field used in this experiment was 1500 V/cm since a 2000-V/cm field was observed to reduce the overall ion-beam current. The static-field plates are connected to ground through high-power resistor banks. The plates are alternately charged and grounded by a pair of high-voltage reed relays that connect and disconnect high-voltage power supplies. This arrangement allows the field to be switched on and off at 10 Hz. Directly after the experimental region, the remaining ions are electrostatically swept out of the beam path and collected in a Faraday cup that provides the ability to measure the beam current at all times. Figure 2 illustrates the deflection and static-field regions.

The undeflected neutral atoms were detected with a Galileo 4821G channeltron operated in pulse-counting mode. The detector entrance was negatively biased to 3500 V in order to achieve the highest range of linearity

and to repel stray electrons. The channeltron was tested over a wide range of input counts with a variety of discriminator settings in order to find the largest region of linearity. The ion-beam current was reduced from hundreds of nanoamperes to 0.5 nA in order to remain well within this range. The linearity of the counting system was further investigated by doubling and halving both the laser power and the ion current separately and together and checking that the signals scaled as expected. In addition, well above threshold, where the oscillations have died out, the field-on to field-off ratio was measured to confirm that it was 1.00. The signal as a function of time after the laser fired was examined to ensure that the background was representative of the collisional stripping. These tests firmly established that, with our operating parameters, the measured backgrounds could be accurately subtracted from the signal bin and that changes in the observed field-on to field-off ratio were truly proportional to changes in the number of neutral atoms.

The channeltron output was capacitively coupled to two Minicircuits ZFL 500-MHz broadband linear amplifiers. Since the amplifiers only respond to signals faster than 50 kHz, baseline drift was not a problem. The amplified signal was sent through a Phillips Scientific Model 6904 300-MHz discriminator to a Joerger Enterprises Inc. Model S3 150-MHz deadtimeless counter. Every 30 sec, the CAMAC controller sent the counter output directly to a computer's hard disk so the data could be analyzed at a later time.

The laser system consists of a Quanta-Ray PDL-1 pulsed dye laser (PDL) pumped by the second harmonic of a Quanta-Ray DCR 2 pulsed Nd:YAG laser. The PDL produced 5-ns full width at half maximum pulses at 20 Hz, with a bandwidth of  $0.4 \text{ cm}^{-1}$ . The  $\text{S}^-$  data were taken with 400–450 mW of laser power, near 600-nm wavelength, generated using Exciton R640 perchlorate dye in methanol. A small amount of acetic acid was added to the solution to shift the power curve of the dye to the red. The 15–24-mW of uv light for the  $\text{Cl}^-$  experiment was produced using a mixture of Exciton DCM and LDS 698 dyes to produce light near 686 nm and then doubling the frequency using a potassium dihydrogen phosphate crystal. The cross section of the laser beam was about  $0.07 \text{ cm}^2$  where it intersected the ion beam. Since no polarization dependence is expected, the light polarization was chosen on the basis of experimental convenience. The  $\text{S}^-$  data were taken with the polarization perpendicular to the electric field, while the  $\text{Cl}^-$  data were taken with the polarization parallel to the field.

The laser was calibrated using a hollow-cathode argon lamp. The argon lines were measured over a wavelength range extending approximately 10 nm above and below the region where the data were taken. A linear calibration was used to compare the measured lines to the reference lines. An absolute calibration of the laser wavelength is only important for determining the location of the photodetachment threshold. The thresholds measured by comparing the *s*-wave Wigner law to the zero-field detachment data are within error of the thresholds determined by using the calibration results and the accepted values for the electron affinities [22,23].

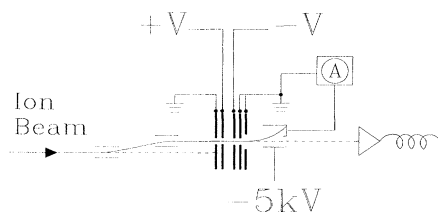


FIG. 2. Side view of the interaction region.

As previously mentioned, above threshold, the data were collected in a manner which is insensitive to temporal variations of the laser and ion beam intensities and to the overlap of the two beams. The laser fires every 50 ms, and beginning with each laser pulse, the data were recorded in 32 1- $\mu$ s-wide time bins. The detachment signal is contained within one bin and the following bins are used to measure the neutral background due to collisional stripping so it can be subtracted out. The data are taken with the electric field on during every other laser shot. Data from 300 laser pulses, taken with the field on, are compared to data from the 300 intervening pulses, taken with the field off. The ratio of detachment signal with the electric field on to that with the field off is measured as a function of laser photon energy and this is directly compared with  $H(E,F)$ . While the ion-beam current and the laser power vary on the time scale of minutes, the variations are very small in a fraction of a second and therefore do not affect the data. Each data point represents 30–60 min of data collection time.

#### IV. OBSERVATIONS

The data obtained for  $\text{Cl}^-$  in 1476-V/cm and 984-V/cm fields are shown in Fig. 3 along with fits to theoret-

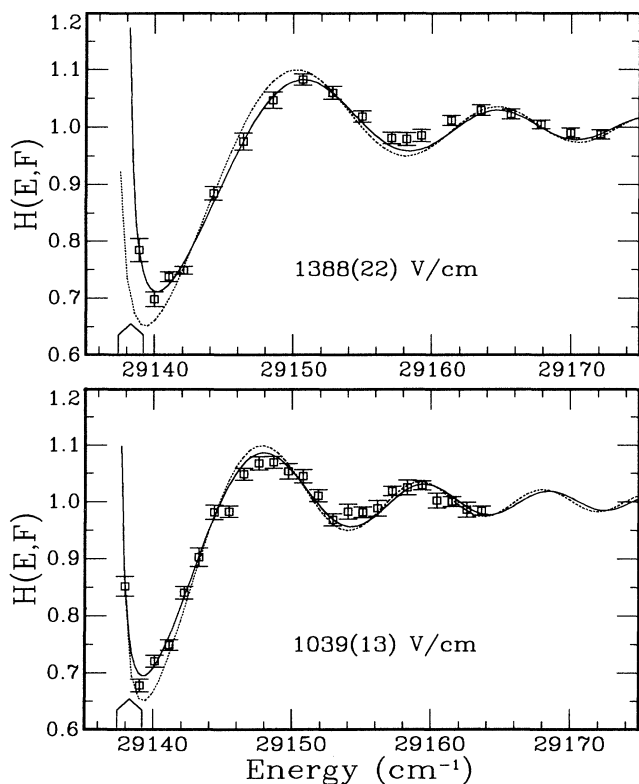


FIG. 3.  $\text{Cl}^-$  data in 1476(29)-V/cm and 984(20)-V/cm applied fields. The dotted curve is  $H(E,F)$  and the solid line is  $H'(E,F,A)$  which includes the amplitude correction. The electric fields fit to 1388(22) V/cm, with an amplitude factor  $A=0.82(2)$ , and to 1039(13) V/cm with  $A=0.86(2)$ . The threshold is shown by the marker and the width of the marker represents the uncertainty in the threshold.

ical models. The positions of the thresholds and the values of the field amplitudes were variable parameters in these fits. The markers along the energy axis indicate the positions of the accepted thresholds and include the quoted errors in the published values, uncertainty in the laser calibrations, and uncertainty from the Doppler shift arising from errors in the perpendicularity of the two beams. Figure 4 shows the corresponding information for  $\text{S}^-$  detachment in 984-V/cm and 492-V/cm electric fields. Upon analyzing the data, it became clear that the phase and periodicity of the oscillations were in good agreement with those predicted by the model but the amplitude of the oscillations was not as great as predicted. In order to investigate the decrease in the amplitude of the oscillations, the model used to fit the data was modified to include an amplitude factor,  $A$ . The data were refit using  $H'=\{1.0+A[H(E,F)-1.0]\}$ . In Figs. 3 and 4, the dotted line shows the result of the fit to  $H(E,F)$  and the solid line shows the result of a fit to  $H'(E,F,A)$ , which includes the amplitude parameter. The ratio cannot be plotted for photon energies below threshold since it diverges as the zero-field detachment goes to zero. Notice that the period of the oscillation increases with increasing field while the amplitude of the oscillation is not obviously dependent on field strength. The agreement between the data and the reduced amplitude theoretical curves is good for both  $\text{S}^-$  and  $\text{Cl}^-$ . Table I provides a summary of the results for electric field and amplitude.

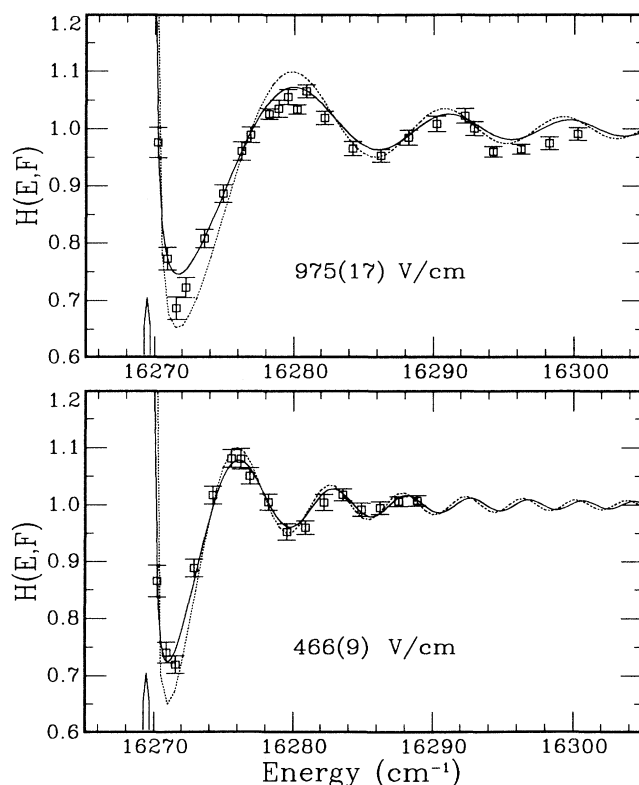


FIG. 4.  $\text{S}^-$  data in 984(20)-V/cm and 492(11)-V/cm fields. The field values fit to 975(17) V/cm with  $A=0.73(2)$  and to 466(9) V/cm with  $A=0.78(3)$ .

TABLE I. Summary of the experimental results. Numbers in parentheses are uncertainty figures.

Applied field (V/cm)	Ion	Fitted field (V/cm)	Amplitude
1476(29)	Cl <sup>-</sup>	1388(22)	0.82(2)
984(20)	Cl <sup>-</sup>	1039(13)	0.86(2)
984(20)	S <sup>-</sup>	975(17)	0.73(2)
492(11)	S <sup>-</sup>	466(9)	0.78(3)

The threshold positions obtained from all of the fits, including the zero-field fits, are within error of the accepted values.

Plots of the 1476-V/cm Cl<sup>-</sup> and 984-V/cm S<sup>-</sup> data below threshold are shown in Fig. 5. The average number of counts per laser shot is the total signal minus the measured stripping signal and the number of background counts measured far below threshold. The squares represent the detachment signal with the field on and the triangles that for the field off. Notice that immediately above threshold, the two curves cross and the "on" signal drops below the "off" signal. This region corresponds to the first dip in  $H(E, F)$ .

The data above and below threshold can be presented together in a plot of the full photodetachment cross section in an electric field. The data taken at energies above

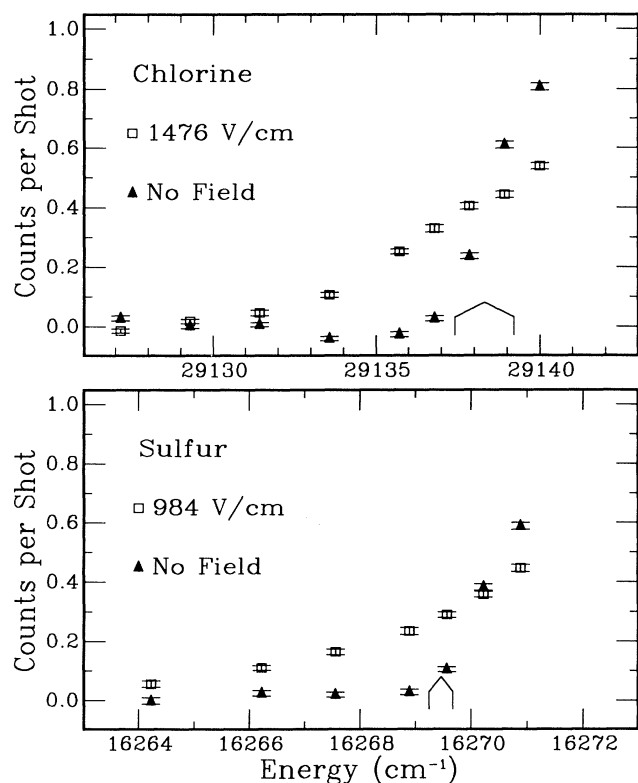


FIG. 5. A plot of the below threshold detachment for Cl<sup>-</sup> and S<sup>-</sup>. The squares represent field-on data and the triangles represent field-off data. Notice that just above threshold, the field-on value is suppressed below the field-off value.

threshold can be displayed as a cross section by simply multiplying the photodetachment ratios by the value of the cross section as given by the Wigner law, with an arbitrary normalization, at each data point. The below threshold data must then be scaled to this cross section. The scale factor was determined by matching an above-threshold cross-section measurement to the Wigner law cross section. Unlike measurements of the ratios, measurements of photodetachment rates are dependent on laser and ion-beam overlap and intensities. Hence, the matching point must be taken immediately after the below threshold scan to ensure that experimental conditions have not changed. By multiplying the below-threshold data by the scale factor thus determined, the full cross section can be displayed in arbitrary units. The resulting cross section is compared to the *s*-wave Wigner law in Fig. 6. The curved line is the undamped function fit to the data taken above threshold only. Notice that the horizontal axes have the same range so a comparison of the oscillation period can be made.

## V. CONCLUSIONS

A careful study of *s*-wave photodetachment in a truly static electric field has been completed. The quality of the data allows the first quantitative test of the theory of photodetachment from negative ions in a static electric

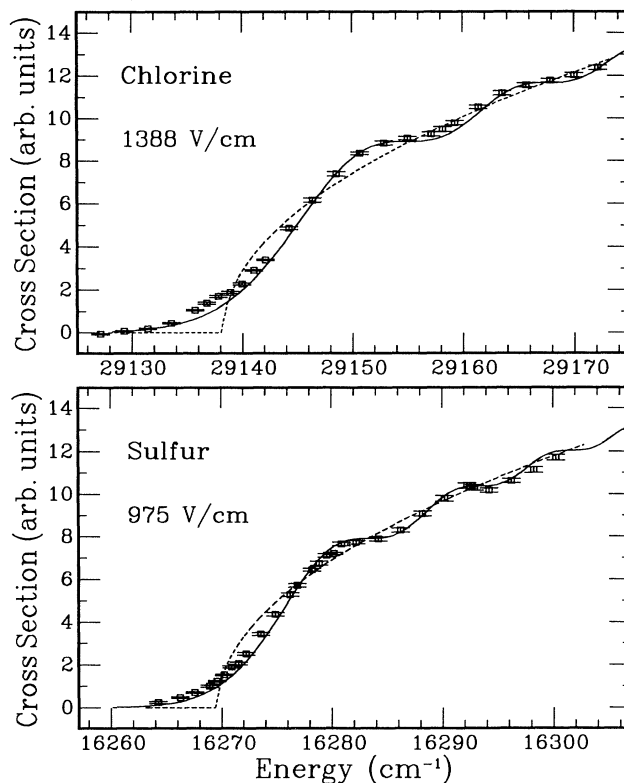


FIG. 6. The Cl<sup>-</sup> and S<sup>-</sup> detachment data plotted around the Wigner law cross section (dashed line) and the undamped electric field cross section (solid line). The field value is only fit to the above threshold points and the below threshold data were matched to the curve as described in the text.

field. In the data of Baruch *et al.*, there appeared to be some discrepancy between the  $\text{Cl}^-$  behavior and the theory near threshold. This discrepancy did not seem to be present in the  $\text{S}^-$  data [20]. We do not find this type of disagreement in  $\text{Cl}^-$  and we do not see any significant differences between the  $\text{S}^-$  and  $\text{Cl}^-$  behaviors. Among the differences between the data for  $\text{S}^-$  and  $\text{Cl}^-$  is that the detaching light was perpendicular to the static field direction for  $\text{S}^-$  and parallel for  $\text{Cl}^-$ .

To a large extent, the data are in good agreement with the theory. The phase of the oscillations appears to be in reasonable agreement with the simple model; the field values obtained from the fits to  $H(E, F, A)$  are all close to the applied field values. These values are presented in Table I. They are neither systematically high nor low. However, the amplitude of the oscillations is reduced to about 80% of the expected value. The data are remarkably consistent in implying a reduced oscillation amplitude.

The possible explanations for the discrepancies between the observed oscillation amplitude and that of the theoretical model may be considered in two categories, experimental and theoretical. Possible experimental effects include the linearity of the detection system and the laser bandwidth and resettability. Since the detection system was carefully tested to ensure linearity, the amplitude of the oscillations does not appear to be affected by a nonlinearity of the detection system. In fact, the most obvious effect of nonlinearity would be the measurement of a background signal that was proportionally higher than the measurement of the detachment signal and that effect would not produce the reduced amplitude that we see here. Overcounting the background would result in the signal appearing smaller than it actually is for both field on and field off. Given that the difference between field on and field off should still be representative of the change in the photodetachment signal,  $H(E, F)$  would be artificially increased for ratios above 1.00 and correspondingly decreased for ratios below 1.00. This is the opposite of the effect observed here.

The finite laser bandwidth produces some averaging over energy values in the measurement of  $H(E, F)$  and this could lead to a reduction in peak height. However, a bandwidth of just over half a wave number would reduce the height of the first maximum in  $H(E, F)$  by only 0.001, which is much less than the observed reduction 0.014–0.027. Additionally, the resettability of the dye laser enters in a similar fashion. Since each data point was measured 2–4 times, and the resettability of the laser is around  $0.2 \text{ cm}^{-1}$ , the effective bandwidth of the light used for each final  $H(E, F)$  measurement is somewhat increased, but this effect is still much too small to account for the observed result.

Another possible explanation for the discrepancy between data and theory is the presence of the Earth's magnetic field. This approximately 1-G field is roughly perpendicular to the electric field in this experiment. A magnetic field alters the path of the outgoing electron and can change the point to which it returns. Anything that randomly changes the phase or reduces the amplitude of the part of the electron wave function that comes

back and interferes will reduce the amplitude of the oscillations. However, the calculations of Du [24] and Fabrikant [25] suggest that a 1-G field should produce little or no effect.

Our theoretical model makes a number of simplifying assumptions that should be considered. A  $\delta$  function is used to represent the interaction of the photon with the initial bound state, thus neglecting the finite size of the binding potential. However, the effect of the finite size was investigated and it was discovered that a 200–300-Å initial bound state range would be needed in order to produce the observed change in the oscillation height. Small amounts of  $d$ -wave detachment have also been neglected by using a  $\delta$  function, and oscillations on the  $d$ -wave cross section could have different amplitudes and phases. Up to  $30 \text{ cm}^{-1}$  above threshold, however, the ratio of  $d$ -wave detachment to  $s$ -wave detachment is only about  $10^{-6}$  and this is far too small to account for the height of the oscillations. The other main assumption is the use of a free-electron wave function for the final state. This neglects the dipole polarizability of the atom and all final-state interactions. The electric field polarizes the electron cloud of the ion before detachment and the neutral atom's cloud after detachment. Since the field-off detachments are not subject to this effect, one would probably expect this effect to produce an overall increase or decrease in  $H(E, F)$  rather than a damping of oscillations but it is difficult to be sure without a more detailed calculation. A related phenomenon is the photodetached electron's interaction with the atomic core. The departing electron also polarizes the neutral but in this case the effect is largely independent of whether the electric field is on or off. The model used here is in very close agreement with the frame transformation calculation of Wong, Rau, and Greene [11] which uses similar assumptions but includes nonzero phase shifts. Fabrikant also includes the effect of nonzero phase shifts in describing rescattering of the electron off the atomic core [9]. However, it is not clear that the inclusion of the phase shifts will completely account for the reduced amplitude of the oscillations.

The previous photodetachment experiments carried out in electric fields do not provide much information about the amplitude of the oscillations. Although Bryant *et al.*, Stewart *et al.*, and Harris *et al.* appear to find reasonable agreement with the theory of Rau and Wong [8], they do not present a clear result for the amplitude of oscillations over the entire range of their data. Also, since the  $\text{H}^-$  data are  $p$ -wave detachment, the effects influencing the oscillation amplitude may be different. Greene and Rouze do not find the predicted oscillation amplitude in the Frey *et al.* data but that is a more complicated case due to the availability of more than one detachment channel. The Baruch *et al.* microwave field data are consistent with the calculated oscillation amplitude. However, the oscillating microwave field results in an average over field values which produces a maximum peak height of 1.04 rather than the static-field peak height of 1.10. Combined with the greater errors in the Baruch *et al.* data, this makes it difficult to quantitatively investigate the peak oscillation height. The data of the

present work consistently exhibit a reduced amplitude. So, there is general agreement between data and calculations for the phase and periodicity of oscillations on the negative-ion photodetachment cross section produced by a static electric field, but the amplitude of these oscillations is not entirely understood and requires further investigation.

#### ACKNOWLEDGMENTS

The authors would like to acknowledge helpful conversations with C. H. Greene and experimental assistance from J. N. Yukich. This work was supported in part by the National Science Foundation.

- 
- [1] E. P. Wigner, *Phys. Rev.* **73**, 1002 (1948).
  - [2] See, for example, W. C. Lineberger, H. Hotop, and T. A. Patterson, *Electron and Photon Interactions with Atoms* (Plenum, New York, 1976), p. 125.
  - [3] F. I. Dalidchik and V. Z. Slonim, *Zh. Eksp. Teor. Fiz.* **70**, 47 (1976) [*Sov. Phys. JETP* **43**, 25 (1976)].
  - [4] Yu. N. Demkov, V. D. Kondratovich, and V. N. Ostrovskii, *Pis'ma Zh. Eksp. Teor. Fiz.* **34**, 425 (1981) [*JETP Lett.* **34**, 403 (1981)].
  - [5] I. I. Fabrikant, *Zh. Eksp. Teor. Fiz.* **83**, 1675 (1982) [*Sov. Phys. JETP* **56**, 967 (1982)].
  - [6] W. P. Reinhardt, in *Atomic Excitations and Recombination in External Fields*, edited by M. H. Nayfeh and C. W. Clark (Gordon and Breach, New York, 1985).
  - [7] I. I. Fabrikant, *Zh. Eksp. Teor. Fiz.* [*Sov. Phys. JETP* **52**, 1045 (1980)].
  - [8] A. R. P. Rau and H.-Y. Wong, *Phys. Rev. A* **37**, 632 (1988).
  - [9] I. I. Fabrikant, *Phys. Rev. A* **40**, 2373 (1989).
  - [10] M. L. Du and J. B. Delos, *Phys. Rev. A* **38**, 5609 (1988).
  - [11] H.-Y. Wong, A. R. P. Rau, and C. H. Greene, *Phys. Rev. A* **37**, 2393 (1988).
  - [12] V. Z. Slonim and C. H. Greene, *Radiat. Eff. Defects Solids* **122&123**, 679 (1991).
  - [13] H. C. Bryant, A. Mohagheghi, J. E. Stewart, J. B. Donahue, C. R. Quick, R. A. Reeder, V. Yuan, C. R. Hummer, W. W. Smith, S. Cohen, W. P. Reinhardt, and L. Overman, *Phys. Rev. Lett.* **58**, 2412 (1987).
  - [14] J. E. Stewart, H. C. Bryant, P. G. Harris, A. H. Mohagheghi, J. B. Donahue, C. R. Quick, R. A. Reeder, V. Yuan, C. R. Hummer, W. W. Smith, and S. Cohen, *Phys. Rev. A* **38**, 5628 (1988).
  - [15] P. G. Harris, H. C. Bryant, A. H. Mohagheghi, C. Tang, J. B. Donahue, C. R. Quick, R. A. Reeder, S. Cohen, W. W. Smith, J. E. Stewart, and C. Johnstone, *Phys. Rev. A* **41**, 5968 (1990).
  - [16] P. Frey, F. Breyer, and H. Hotop, *J. Phys. B* **11**, L589 (1978).
  - [17] P. Frey, M. Lawen, F. Breyer, H. Klar, and H. Hoptop, *Z. Phys. A* **304**, 155 (1982); **306**, 185E (1982).
  - [18] C. H. Greene and N. Rouze, *Z. Phys. D* **9**, 219 (1988).
  - [19] M. C. Baruch, T. F. Gallagher, and D. J. Larson, *Phys. Rev. Lett.* **65**, 1336 (1990).
  - [20] M. C. Baruch, W. G. Sturru, N. D. Gibson, and D. J. Larson, *Phys. Rev. A* **45**, 2825 (1992).
  - [21] R. Middleton, "A Negative-Ion Cookbook" University of Pennsylvania report, 1990 (unpublished).
  - [22] R. Trainham, G. D. Fletcher, and D. J. Larson, *J. Phys. B* **20**, L777 (1987).
  - [23] Chris Edge, thesis, University of Virginia, 1988 (unpublished).
  - [24] M. L. Du, *Phys. Rev. A* **40**, 1330 (1989).
  - [25] I. I. Fabrikant, *Phys. Rev. A* **43**, 258 (1991).